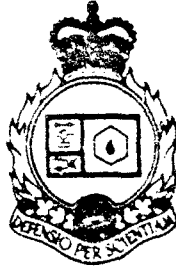


DTIC FILE COPY

①



National Defence / Defense nationale



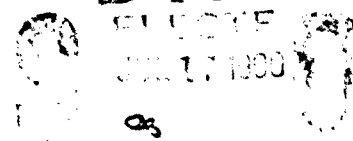
THE VALIDITY OF THE USE OF THE NEUTRON REDUCTION FACTOR IN ASSESSING DISPLACEMENT DAMAGE TO ELECTRONICS IN ARMoured VEHICLES

by

T. Cousins and T.J. Jamieson

AD-A223 878

DTIC



20030206122

DEFENCE RESEARCH ESTABLISHMENT OTTAWA
REPORT NO.1032

Canada



February 1990
Ottawa

90 07 16 306



National
Defence

Defense
nationale

**THE VALIDITY OF THE USE OF THE NEUTRON
REDUCTION FACTOR IN ASSESSING
DISPLACEMENT DAMAGE TO ELECTRONICS
IN ARMoured VEHICLES**

by

T. Cousins
Nuclear Effects Section
Electronics Division

and

T.J. Jamieson
Science Applications International Corporation (SAIC Canada)
Ottawa, Ontario

DEFENCE RESEARCH ESTABLISHMENT OTTAWA

REPORT NO.1032

PCN
041LS

February 1990
Ottawa

ABSTRACT

The degree of protection from neutron irradiation afforded to electronics by armoured vehicles is most correctly defined by the outside-to-inside ratio of the 1 MeV equivalent neutron fluence for Silicon. It has been proposed that this factor may be approximated by an experimentally measurable parameter - the neutron (tissue kerma) reduction factor. This report examines the validity of this assumption for a variety of realistic nuclear battlefield scenarios, calculated using the computer code VPF2. In addition the response of two neutron dosimeters in the calculated fields is examined.

RESUME

Le degré de protection des composantes électroniques contre les irradiations de neutrons reçues est correctement défini par le rapport de pénétration extérieur-vers-l'intérieur de 1 MeV équivalent de fluence silicium. Il a été proposé que facteur pouvait être représenté par un paramètre mesurable, le facteur de réduction de neutron (tissue kerma). Ce rapport étudie la validité de cette hypothèse pour une variété de scénarios possibles en utilisant le programme VPF2. De plus, la réponse de deux dosimètres de neutrons est étudiée.

| | |
|--------------------|-------------------------------------|
| Accession For | |
| NTIS GRA&I | <input checked="" type="checkbox"/> |
| DTIC TAB | <input type="checkbox"/> |
| Unannounced | <input type="checkbox"/> |
| Justification | |
| Distribution Codes | |
| Distribution Code/ | |
| Distribution Code | |



A-1

EXECUTIVE SUMMARY

In order to predict the degree of protection afforded to electronics by armoured vehicles exposed to neutron irradiation, the ratio of outside to inside tissue kermas has often been used as an approximation. This report examines the validity of this approximation by using the computer code VPF2 to generate neutron fields to be expected in a number of battlefield scenarios. The performance of two neutron dosimeters in these fields is also examined.

TABLE OF CONTENTS

| | <u>PAGE</u> |
|--|-------------|
| ABSTRACT/RÉSUMÉ | iii |
| EXECUTIVE SUMMARY | v |
| TABLE OF CONTENTS | vii |
| LIST OF TABLES AND FIGURES | ix |
| | |
| 1.0 <u>INTRODUCTION</u> | 1 |
| | |
| 2.0 <u>METHODOLOGY</u> | 2 |
| 2.1 Definition of Factors | 2 |
| 2.2 Computer Codes | 3 |
| 2.3 Weapon Specifications | 3 |
| 2.4 Vehicle Types | 4 |
| 2.5 Dosimeter Response | 5 |
| | |
| 3.0 <u>RESULTS</u> | 5 |
| 3.1 Experimental Results | 5 |
| 3.2 Calculational Results | 6 |
| 3.2.1 Free-Field Ranges and Spectra | 6 |
| 3.2.2 Dosimeter Response | 7 |
| | |
| 4.0 <u>CONCLUSIONS AND RECOMMENDATIONS</u> | 13 |
| | |
| APPENDIX A | 21 |
| | |
| APPENDIX B | 22 |
| | |
| 5.0 <u>BIBLIOGRAPHY</u> | 25 |

LIST OF TABLES AND FIGURES

| | <u>Page</u> |
|----------------|--|
| <u>TABLES</u> | |
| TABLE 1 | Simulated Vehicle Types 4 |
| TABLE 2 | Results from Test Bed Experiments and Calculations 6 |
| TABLE 3 | Ranges for Stated Effect 7 |
| TABLE 4 | Dosimeter Responses (rads) in SFW Environments 8 |
| TABLE 5 | Dosimeter Responses (rads) in TNW Environments 9 |
| TABLE 6 | Dosimeter Response in 14 MEV Environments 10 |
| TABLE 7 | Comparison of ORF to NRF Values 12 |
| <u>FIGURES</u> | |
| FIGURE 1 | VPF2 Methodology 14 |
| FIGURE 2 | BD100R fluence/energy response used in this report. 15 |
| FIGURE 3 | Measured (ROSPEC) neutron energy spectra both free-field (at the NATO standard reference point) and in the test bed configuration. 16 |
| FIGURE 4 | Ratio of neutron tissue kerma to neutron displacement kerma in Si. Note the structure riding on a fairly flat base. 17 |
| FIGURE 5 | Free field neutron energy spectra (for the ITI case) as calculated by ATR5 for the three weapon scenarios. 18 |
| FIGURE 6 | Ratio of bubble response per neutron tissue kerma showing a large peaking in the area of 300-400 keV. 19 |
| FIGURE 7 | Free-field (ITI) and V2 neutron energy spectra for the TNW scenario as calculated by VPF2. Note the maximum in the V2 spectra is a roughly the same energy as the peak in the bubble per tissue kerma curve (Figure 6). This is responsible for the high values for bubble detector measured kerma predicted in the text. 20 |

1.0 INTRODUCTION

The protection factor afforded by armoured vehicles to the deleterious effects of radiation from nuclear weapons is a subject of much concern to the NATO community - so much so that it has spawned an entire Allied Engineering Publication (AEP-14) (1). While the document is extremely thorough in addressing the issue of protection of personnel, only minor mention is made of the protection afforded to electronics. In particular, when considering the damage created by neutron irradiation of semiconductors, the concept of 1 MeV equivalent neutron fluence is generally used (2). AEP-14 states only that the neutron protection afforded to electronics may be approximated by the neutron reduction factor - which is essentially a ratio of tissue kerma. This work strives to examine the validity of this approximation for a variety of battlefield scenarios using the latest DREO-developed computational capabilities.

2.0 METHODOLOGY

2.1 DEFINITION OF FACTORS

The characterization of radiation protection factors afforded by armoured vehicles necessitates the definition of a number of protection factors. These are all based on the neutron and gamma-ray energy spectra both inside and outside the vehicle being convolved with an appropriate response function, and the subsequent evaluation of their ratio, i.e.

$$(XPF)_R = \frac{\int \phi_{\text{outside}}(E) R(E) dE}{\int \phi_{\text{inside}}(E) R(E) dE} \quad (1)$$

where

$(XPF)_R$ = general protection factor for parameter
having energy response $R(E)$

$\phi_{\text{inside}}(E)$ = particle fluence inside vehicle

$\phi_{\text{outside}}(E)$ = particle fluence outside vehicle

Based on the general definition of (1), any protection factor may be calculated. From AEP-14 the most commonly used factors - namely the neutron and gamma-ray reduction and protection factors (in which $R(E)$ is the tissue kerma response function) are defined as:

(i) Gamma-Ray Protection Factor

$$GPF = \frac{\text{Gamma Ray Kerma Outside Vehicle}}{\text{Kerma Due to Gamma Rays Penetrating Vehicle}} \quad (2)$$

(ii) Neutron Protection Factor

$$NPF = \frac{\text{Neutron Kerma Outside Vehicle}}{\text{Neutron Kerma Inside Vehicle + Armour-generated Secondary Gamma Ray Kerma}} \quad (3)$$

(iii) Gamma-Ray Reduction Factor

$$\text{GRF} = \frac{\text{Gamma-Ray Kerma Outside Vehicle}}{\text{Gamma-Ray Kerma Inside Vehicle}} \quad (4)$$

(iv) Neutron Reduction Factor

$$\text{NRF} = \frac{\text{Neutron Kerma Outside Vehicle}}{\text{Neutron Kerma Inside Vehicle}} \quad (5)$$

For neutron irradiation of semiconductor materials, the major damage-causing mechanism is displacement of silicon atoms due to elastic (and inelastic) collisions. Thus the Silicon Displacement Kerma energy response is the important parameter as $R(E)$ in eqn(1). However the normal procedure for characterizing semiconductor damage is to reduce the neutron fluence to the equivalent fluence of 1 MeV neutrons (2), i.e.

$$\phi_{\text{eq}}(1 \text{ MeV}) = \frac{\int \phi(E) K_D(E) dE}{K_D(1 \text{ MeV})} \quad (6)$$

where

$\phi_{\text{eq}}(1 \text{ MeV})$ - 1 MeV equivalent neutron damage in Si

$K_D(E)$ - neutron displacement kerma factor for Si

$K_D(1 \text{ MeV})$ - neutron displacement kerma factor for 1 MeV neutrons

$$= (3.26 \pm 0.14) \times 10^{-11} \text{ Rad-cm}^2 \quad (3)$$

Calculation of the 1 MeV equivalent neutron fluence allows definition of the 1 MeV equivalent neutron reduction factor as:

$$\text{CRF} = \frac{\int \phi_{\text{outside}}(E) Y_D(E) dE}{\int \phi_{\text{inside}}(E) Y_D(E) dE} \quad (7)$$

The comparison of the CRF (which is the direct measure of the effectiveness of vehicle shielding for neutron damage to electronics) to NRF (which is an experimentally measurable approximation) is the main thrust of this work

Of course, knowledge of the both inside and outside energy spectra allows direct evaluation of dosimeter performance and many other relevant parameters some of which will be glanced upon here.

2.2 COMPUTER CODES

In order to evaluate the inside and outside energy spectra at realistic distances from simulated nuclear weapons the computer code VPF2 (4) (in a slightly modified form) was used. The code is micro-computer based and menu driven. It uses an interface with another code - ATR5 (5) - to generate two-dimensional angular fluence data at the vehicle range.

The two-dimensional data is then collapsed into effective one-dimensional fluences which are then used as a source term for ANISN slab radiation transport calculations into the vehicle. As a result the protection and reduction factors calculated by VPF2 are effectively averaged over all azimuthal vehicle orientations within the free-field.

For this work, a special modification of VPF2 allowing particle energy spectra output was employed.

Fig (1) should clarify the VPF2 methodology.

2.3 WEAPON SPECIFICATIONS

To make the comparisons meaningful, the entire gamut of energy spectra likely to be encountered on the battlefield should be covered. To accomplish this, three separate source spectra were employed. They were:

- (a) The standard fission weapon (SFW) source spectrum from ATR5
 - (b) The thermonuclear weapon (TNW) source spectrum from ATR5
 - (c) A source consisting entirely of 14 MeV neutrons (14 MeV)
- Appendix (A) lists source spectra (a) and (b).

The yields chosen here were 5 kT and 100 kT for each weapon, with the source normalizations being 2×10^{23} n/kT and 5×10^{22} g/kT for the SFW case and 1.2×10^{24} n/kT for the TNW and 14 MeV cases. No gamma-ray source term was used with either the TNW or 14 MeV cases since recent DREO calculations have shown (6) that the contribution to total dose from prompt gamma rays is generally dwarfed by that from neutron-capture gamma rays.

The height-of-burst (HOB) for the weapons were chosen as that which would maximize blast effects, i.e.

$$HOB = 60 (\text{YIELD})^{1/3} \quad (8)$$

Thus the HOBs were 102.6 m and 278.5 m for the 5 kT and 100 kT bursts respectively.

The air-over-ground calculations used the default air and ground elemental composition and moisture content from ATR5.

The dose constraint option within ATR5 was used to give the ranges from the weapons at which free-field neutron tissue kerms of 450 Rads (LD_{50}) and 2500 Rads (ITI) would occur. The vehicle was then placed at these ranges and the VPF2 calculations commenced.

2.4 VEHICLE TYPES

Since the purpose of this report was chiefly to compare ORF to NRF, which are ratios, it was decided that extremely simplistic vehicles would suffice. However these model vehicles would need enough detail to show broad differences in vehicle design, such as thin-walled (APC) vs thick-walled (tank) vehicles with

and without the addition of a liner. Accordingly the vehicle types described in table (1) were employed. All are a simple 2m x 2m x 2m (outside dimensions) cube.

TABLE 1
SIMULATED VEHICLE TYPES

| CODE | DESCRIPTION |
|------|--|
| V1 | 2" thick Al walls |
| V2 | 6" thick steel walls |
| V3 | 2" thick Al walls with 2" thick polyethylene liner on inside |
| V4 | 6" thick steel walls with 2" thick polyethylene liner on inside |

2.5 DOSIMETER RESPONSE

The calculation of the response of a dosimeter in an arbitrary field depends upon knowledge of the radiation energy spectrum in that field, plus the energy spectrum of the radiation field in which the dosimeter was calibrated.

Then defining R_{cal} and K_{cal} as the detector response and tissue kerma, respectively, in the calibration field, i.e.

$$R_{cal} = \int \phi_{cal}(E) R_D(E) dE \quad (9)$$

$$K_{cal} = \int \phi_{cal}(E) K_T(E) dE \quad (10)$$

where

ϕ_{cal} = radiation fluence in calibration field

$R_D(E)$ = energy-dependent detector response (arbitrary units)

$K_T(E)$ = energy-dependent tissue kerma response

Then one may define a calibration factor, C, as

$$C = K_{cal}/R_{cal} \quad (11)$$

Now when the dosimeter is exposed to an arbitrary fluence field, $\phi_{field}(E)$, the measured response (again in arbitrary units) will be

$$M = \int \phi_{field}(E) R_D(E) dE \quad (12)$$

Then the 'dose' (K_D) indicated by the dosimeter is simply

$$K_D = C M \quad (13)$$

A comparison of K_D with the true radiation field tissue kerma (i.e. replace 'cal' with 'field' in eqn (10)) gives the efficacy of the dosimeter in that particular field.

It was decided here to examine the responses of two neutron dosimeters in the calculated fields. They are the proposed CF neutron dosimeter (which is a Silicon diode(7)) and the super-heated drop or 'bubble' dosimeter (8) which has become DREO's principal experimental neutron dosimeter over the past few years and which, in the future, may see direct military applications. Each dosimeter deserves some further discussion.

For the case of the diode, the detector response function was assumed to be identical to the silicon displacement kerma(9) - which merely assumes that there is little detector escape probability. The calibration factor is then simply the ratio of the energy weighted tissue kerma response to the energy weighted silicon displacement kerma response in the calibration field.

When considering the bubble detector the energy response, as obtained by the manufacturer (10), as shown in fig(2) was used.

The choice of an appropriate calibration field is somewhat arbitrary. Here a ^{252}Cf fission source is assumed - although other common sources such as Pu-Be would not change the results greatly. The ^{252}Cf source has the distinct advantage of a well-defined semi-empirical fit to its energy distribution (the Watt spectrum) as

$$\phi_{\text{cf}}(E) = 0.373 \exp(-0.88E) \sinh(\sqrt{2E}) \text{ n cm}^{-2} \text{ s}^{-1} \text{ MeV}^{-1} \quad (14)$$

Using these the derived calibration factors are

$$C(\text{diode}) = 74.6 \pm 3.2 \text{ Rad(tissue)/Rad(Silicon)} \quad (15)$$

$$C(\text{bubble}) = 9.31 \times 10^{-3} \pm 10\% \text{ Rad(tissue)/bubble} \quad (16)$$

3.0 RESULTS

3.1 EXPERIMENTAL RESULTS

Owing to the lack of sophisticated neutron spectroscopic equipment, experimental data on NRF and ORF is very limited. However one recent experiment at Aberdeen Proving Ground (APG) used the most sophisticated neutron spectrometer (ROSPEC) available for free-field and in-vehicle work (11). Here the neutron spectra were measured at the NATO standard reference point - 400 m from the critical facility core both free-field and in the 'NATO standard test bed' (12). The test bed is actually a 2m x 2m x 2m cube having 4" thick steel walls.

The results of this work are presented in table (2), together with calculational results from VPF2 and more exotic codes.

TABLE 2
RESULTS FROM TEST BED EXPERIMENTS AND CALCULATIONS

| METHOD | NRF | GRF |
|-----------------------|------|------|
| ROSPEC | 1.48 | 1.43 |
| VPF2* | 1.78 | |
| SAIC calculations(13) | 1.60 | |
| ORNL calculations(13) | 1.58 | |
| ETCA calculations(13) | 1.44 | |

*VPF2 results modified to reflect internal scattering

The VPF2 and other calculations used an old source term and the air and ground moisture were not matched to those present during the experimental measurements. The ratio of calculation to experiment for the four cases is (1.08 +/- .09), which gives some confidence to the results to be presented.

The ROSPEC-measured spectra for both inside and outside cases are shown in fig (3). They may both be considered as degraded fission spectra with mean energies of 0.50 and 0.77 MeV respectively. The comparison here between GRF and NRF is excellent - within 3%. This agreement may have been expected when one examines fig (4) - a ratio of the tissue- and silicon displacement kerma factors. The overall trend is reasonably flat here. Still there exists enough structure that some spectral variations in the GRF approximation to NRF may occur, making this study important.

3.2 CALCULATIONAL RESULTS

3.2.1 FREE-FIELD RANGES AND SPECTRA

The ranges at which the ATR5 calculations yielded the LD50 and ITI neutron kermas appear in table (3). Some of the free-field spectra appear in fig (5).

TABLE 3

RANGES FOR STATED EFFECT

| WEAPON | RANGE (m) | |
|---------------|-----------|--------|
| | LD50 | ITI |
| SFW - 5 kT | 970.5 | 750 |
| SFW - 100 kT | 1430.5 | 1177 |
| TNW - 5 kT | 1289.2 | 1015.8 |
| TNW - 100 kT | 1845.6 | 1545.9 |
| 14 MeV- 5 kT | 1579.8 | 1280.7 |
| 14 MeV-100 kT | 2166.8 | 1851 |

3.2.2 DOSIMETER RESPONSE

Tables (4), (5) and (6) give the predicted dosimeter responses for the neutron diode and bubble detectors (as compared to free-field) for the SFW, TNW and 14 MeV cases respectively. Listing of some of the calculated energy spectra appear in Appendix B.

TABLE 4

DOSIMETER RESPONSES(rads) IN SFW ENVIRONMENTS

5 kt weapon
(a) NOMINAL LD50 RANGE

| CASE | TISSUE | N-DIODE | RATIO* | BUBBLE | RATIO* |
|------|--------|---------|------------|--------|-------------|
| FF | 446 | 427 | 0.96 | 641 | 1.43 |
| V1 | 324 | 308 | 0.95 | 459 | 1.42 |
| V2 | 115 | 113 | 0.98 | 207 | 1.80 |
| V3 | 63.8 | 62.5 | 0.98 | 77.6 | 1.22 |
| V4 | 12.9 | 12.4 | 0.96 | 19.4 | 1.56 |
| MEAN | | | .97+/- .01 | | 1.49+/- .21 |

(b) NOMINAL ITI RANGE

| CASE | TISSUE | N-DIODE | RATIO* | BUBBLE | RATIO |
|------|--------|---------|------------|--------|-------------|
| FF | 2480 | 2370 | 0.95 | 3640 | 1.47 |
| V1 | 1800 | 1710 | 0.95 | 2600 | 1.44 |
| V2 | 648 | 633 | 0.98 | 1170 | 1.80 |
| V3 | 339 | 331 | 0.98 | 423 | 1.25 |
| V4 | 70.6 | 67.7 | 0.96 | 108 | 1.52 |
| MEAN | | | .96+/- .02 | | 1.50+/- .20 |

100 kt weapon
(a) NOMINAL LD50 RANGE

| CASE | TISSUE | N-DIODE | RATIO* | BUBBLE | RATIO |
|------|--------|---------|------------|--------|-------------|
| FF | 447 | 431 | 0.96 | 605 | 1.35 |
| V1 | 329 | 316 | 0.96 | 441 | 1.34 |
| V2 | 113 | 111 | 0.98 | 199 | 1.76 |
| V3 | 74.3 | 72.9 | 0.98 | 84.8 | 1.14 |
| V4 | 13.9 | 13.4 | 0.96 | 20.1 | 1.45 |
| MEAN | | | .97+/- .01 | | 1.41+/- .22 |

(b) NOMINAL ITI RANGE

| CASE | TISSUE | N-DIODE | RATIO* | BUBBLE | RATIO |
|------|--------|---------|------------|--------|-------------|
| FF | 2480 | 2380 | 0.96 | 3470 | 1.40 |
| V1 | 1820 | 1740 | 0.96 | 2510 | 1.37 |
| V2 | 636 | 621 | 0.97 | 1130 | 1.78 |
| V3 | 381 | 374 | 0.98 | 450 | 1.18 |
| V4 | 74.2 | 71.3 | 0.96 | 110 | 1.48 |
| MEAN | | | .97+/- .01 | | 1.44+/- .22 |

* RATIOS OF DOSIMETER READINGS TO FF KERMA

TABLE 5

DOSIMETER RESPONSES(RADS) IN TNW ENVIONMENTS

5 kT weapon

(a) NOMINAL LD50 RANGE

| CASE | TISSUE | N-DIODE | RATIO BUBBLE | RATIO | |
|------|--------|---------|--------------|-------|-------------|
| FF | 449 | 433 | 0.96 | 511 | 1.14 |
| V1 | 337 | 324 | 0.96 | 387 | 1.15 |
| V2 | 110 | 108 | 0.98 | 180 | 1.64 |
| V3 | 109 | 105 | 0.96 | 105 | 0.96 |
| V4 | 18.8 | 17.9 | 0.95 | 23.1 | 1.23 |
| | | MEAN | 0.96+/- .01 | | 1.22+/- .25 |

(b) NOMINAL ITI RANGE

| CASE | TISSUE | N-DIODE | RATIO BUBBLE | RATIO | |
|------|--------|---------|--------------|-------|-------------|
| FF | 2610 | 2500 | 0.96 | 2990 | 1.14 |
| V1 | 1940 | 1860 | 0.96 | 2250 | 1.16 |
| V2 | 643 | 629 | 0.98 | 989 | 1.54 |
| V3 | 625 | 599 | 0.95 | 603 | 0.96 |
| V4 | 110 | 105 | 0.95 | 134 | 1.21 |
| | | MEAN | 0.96+/- .01 | | 1.19+/- .20 |

100 kT weapon

(a) NOMINAL LD50 RANGE

| CASE | TISSUE | N-DIODE | RATIO BUBBLE | RATIO | |
|------|--------|---------|--------------|-------|-------------|
| FF | 449 | 435 | 0.97 | 501 | 1.11 |
| V1 | 340 | 329 | 0.97 | 382 | 1.12 |
| V2 | 109 | 107 | 0.98 | 178 | 1.63 |
| V3 | 112 | 108 | 0.96 | 107 | 0.96 |
| V4 | 18.6 | 17.8 | 0.96 | 23 | 1.23 |
| | | MEAN | .97+/- .01 | | 1.21+/- .25 |

(b) NOMINAL ITI RANGE

| CASE | TISSUE | N-DIODE | RATIO BUBBLE | RATIO | |
|------|--------|---------|--------------|-------|-------------|
| FF | 2500 | 2410 | 0.96 | 2800 | 1.12 |
| V1 | 1890 | 1820 | 0.96 | 2130 | 1.12 |
| V2 | 608 | 597 | 0.98 | 989 | 1.62 |
| V3 | 620 | 598 | 0.96 | 594 | 0.96 |
| V4 | 104 | 99.4 | 0.95 | 128 | 1.23 |
| | | MEAN | .96+/- .01 | | 1.21+/- .24 |

TABLE 6
DOSIMETER RESPONSE IN 14 MEV ENVIRONMENT

5 kT weapon

(a) NOMINAL LD50 RANGE

| CASE | TISSUE | N-DIODE | RATIO BUBBLE | RATIO | |
|------|--------|---------|--------------|-------|-------------|
| FF | 450 | 432 | 0.96 | 475 | 1.05 |
| V1 | 340 | 327 | 0.96 | 366 | 1.07 |
| V2 | 109 | 106 | 0.97 | 172 | 1.57 |
| V3 | 123 | 117 | 0.95 | 112 | 0.91 |
| V4 | 20.8 | 19.6 | 0.94 | 24.1 | 1.16 |
| MEAN | | | .96+/- .01 | | 1.15+/- .25 |

(b) NOMINAL ITI RANGE

| CASE | TISSUE | N-DIODE | RATIO BUBBLE | RATIO | |
|------|--------|---------|--------------|-------|-------------|
| FF | 2610 | 2500 | 0.96 | 2990 | 1.19 |
| V1 | 1880 | 1800 | 0.95 | 1990 | 1.06 |
| V2 | 602 | 588 | 0.97 | 941 | 1.56 |
| V3 | 702 | 665 | 0.94 | 631 | 0.89 |
| V4 | 121 | 113 | 0.93 | 136 | 1.12 |
| MEAN | | | .95+/- .02 | | 1.16+/- .25 |

100 kT weapon

(a) NOMINAL LD50 RANGE

| CASE | TISSUE | N-DIODE | RATIO BUBBLE | RATIO | |
|------|--------|---------|--------------|-------|-------------|
| FF | 449 | 434 | 0.97 | 483 | 1.07 |
| V1 | 341 | 330 | 0.96 | 372 | 1.09 |
| V2 | 108 | 106 | 0.98 | 174 | 1.61 |
| V3 | 119 | 114 | 0.96 | 111 | 0.93 |
| V4 | 19.6 | 18.7 | 0.95 | 23.5 | 1.19 |
| MEAN | | | .96+/- .01 | | 1.17+/- .25 |

(b) NOMINAL ITI RANGE

| CASE | TISSUE | N-DIODE | RATIO BUBBLE | RATIO | |
|------|--------|---------|--------------|-------|-------------|
| FF | 2490 | 2400 | 0.96 | 2640 | 1.06 |
| V1 | 1890 | 1820 | 0.96 | 2040 | 1.08 |
| V2 | 600 | 588 | 0.98 | 952 | 1.59 |
| V3 | 679 | 649 | 0.95 | 623 | 0.92 |
| V4 | 113 | 107 | 0.95 | 132 | 1.16 |
| MEAN | | | .96+/- .01 | | 1.16+/- .25 |

The two main features evident from the preceding tables are (a) the excellent performance of the neutron-diode and (b) the poor performance of the bubble dosimeter. The first feature may be attributed to statistically negligible spectral changes when considering the different environments or, should such differences exist, their masking by energy-binning effects. In either case, the neutron-diode is an extremely accurate dosimeter for these fields.

The case of the bubble detector deserves more discussion. The reason for the wide variations from tissue kerma may be grasped from an examination of fig(6). Here the dosimeter response is plotted in a more appropriate fashion as a ratio of expected bubbles per tissue kerma. Note the large peaking in the region around a few hundred keV. Now consider fig(7) in which the free-field and V2 cases for the TNW are shown. The free-field spectrum is relatively flat and the predicted bubble response is close (within 12 %) to tissue kerma. However for the shielded case, the spectrum is highly peaked, unfortunately in the same energy region as the bubble detector response peak - leading to a 60 % over-estimate in kerma.

However, actual experimental data with the bubble detector does not back these results. Take the APG experiments mentioned earlier. Bubble detectors were deployed for this work. The measured responses were 3.83 and 2.78 mRad/kWh for the free-field and in-box cases respectively(11). Using the same procedure as above(i.e using the ROSPEC measured spectra as the input energy spectra and folding into the bubble detector energy-fluence response) the predicted bubble detector kermas would be 7.63 and 6.66 mrad/kWh respectively. The measured NRF would then be 1.38 as compared to the calculated 1.15. This, and other reliable experimental work with the bubble detectors, suggests that the energy response function is not accurate, and more work needs to be done in this area.

Clearly, with the excellent agreement between the neutron-diode response and tissue kerma, the CRF/NRF approximation must be extremely good here. Table (7) merely reinforces this point.

TABLE 7

COMPARISON OF ORF TO NRF VALUES

| SFW WEAPON - LD50 RANGE | | | | |
|-------------------------|------|------|--------|------|
| | 5 kT | | 100 kT | |
| | NRF | ORF | NRF | ORF |
| V1 | 1.38 | 1.39 | 1.36 | 1.36 |
| V2 | 3.87 | 3.78 | 3.94 | 3.88 |
| V3 | 6.99 | 6.82 | 6.02 | 5.91 |
| V4 | 34.5 | 34.3 | 32.1 | 32.1 |

| SFW WEAPON - ITI RANGE | | | | |
|------------------------|------|------|--------|------|
| | 5 kT | | 100 kT | |
| | NRF | ORF | NRF | ORF |
| V1 | 1.38 | 1.39 | 1.36 | 1.37 |
| V2 | 3.83 | 3.75 | 3.9 | 3.83 |
| V3 | 7.34 | 7.17 | 6.51 | 6.37 |
| V4 | 35.2 | 35.1 | 33.4 | 33.4 |

| TNW WEAPON - LD50 RANGE | | | | |
|-------------------------|------|------|--------|------|
| | 5 kT | | 100 kT | |
| | NRF | ORF | NRF | ORF |
| V1 | 1.33 | 1.33 | 1.32 | 1.32 |
| V2 | 4.07 | 4.00 | 4.11 | 4.06 |
| V3 | 4.13 | 4.13 | 4.00 | 4.02 |
| V4 | 23.9 | 24.2 | 24.1 | 24.4 |

| TNW WEAPON - ITI RANGE | | | | |
|------------------------|------|------|--------|------|
| | 5 kT | | 100 kT | |
| | NRF | ORF | NRF | ORF |
| V1 | 1.34 | 1.34 | 1.32 | 1.32 |
| V2 | 4.05 | 3.97 | 4.11 | 4.04 |
| V3 | 4.17 | 4.17 | 4.03 | 4.04 |
| V4 | 23.6 | 23.9 | 23.9 | 24.3 |

| 14 MEV WEAPON - LD50 RANGE | | | | |
|----------------------------|------|------|--------|------|
| | 5 kT | | 100 kT | |
| | NRF | ORF | NRF | ORF |
| V1 | 1.32 | 1.32 | 1.32 | 1.32 |
| V2 | 4.14 | 4.05 | 4.14 | 4.08 |
| V3 | 3.67 | 3.69 | 3.78 | 3.80 |
| V4 | 21.7 | 22.0 | 22.9 | 23.3 |

TABLE 7 (Continued)
COMPARISON OF ORF TO NRF VALUES

| | 14 MEV WEAPON - ITI RANGE | | | |
|----|---------------------------|-------------|------|---------------|
| | NRF | 5 kT ORF | NRF | 100 kT ORF |
| V1 | 1.33 | 1.32 | 1.32 | 1.32 |
| V2 | 4.15 | 4.05 | 4.16 | 4.09 |
| V3 | 3.56 | 3.58 | 3.67 | 3.70 |
| V4 | 20.7 | 21.0 | 22.1 | 22.5 |

4. CONCLUSIONS AND RECOMMENDATIONS

The use of the neutron reduction factor as a means of estimating the silicon displacement damage to semiconductors has been proven valid for a variety of cases. As an additional output of this work the efficacy of the neutron diode dosimeter in these fields has also been demonstrated. The absolute value and shape of the bubble dosimeter energy response is brought into question by the theoretical and experimental results presented here.

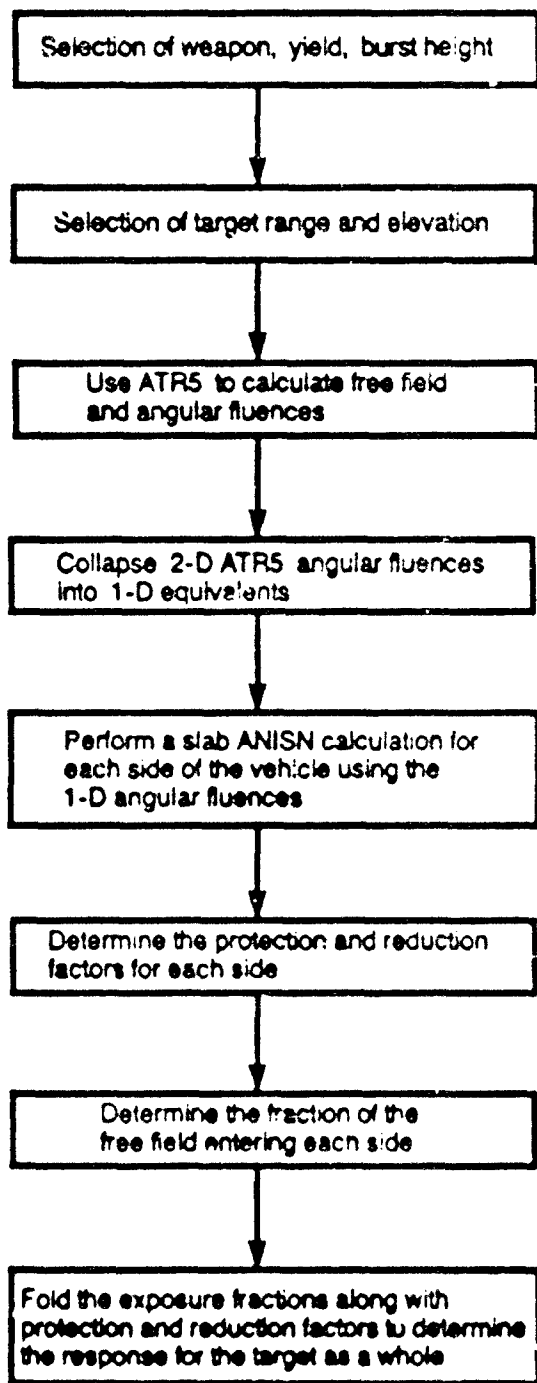


FIGURE 1 VPF2 Methodology

BD100 R RESPONSE USED IN THIS REPORT FROM DREO VAN DE GRAAFF EXPERIMENTS

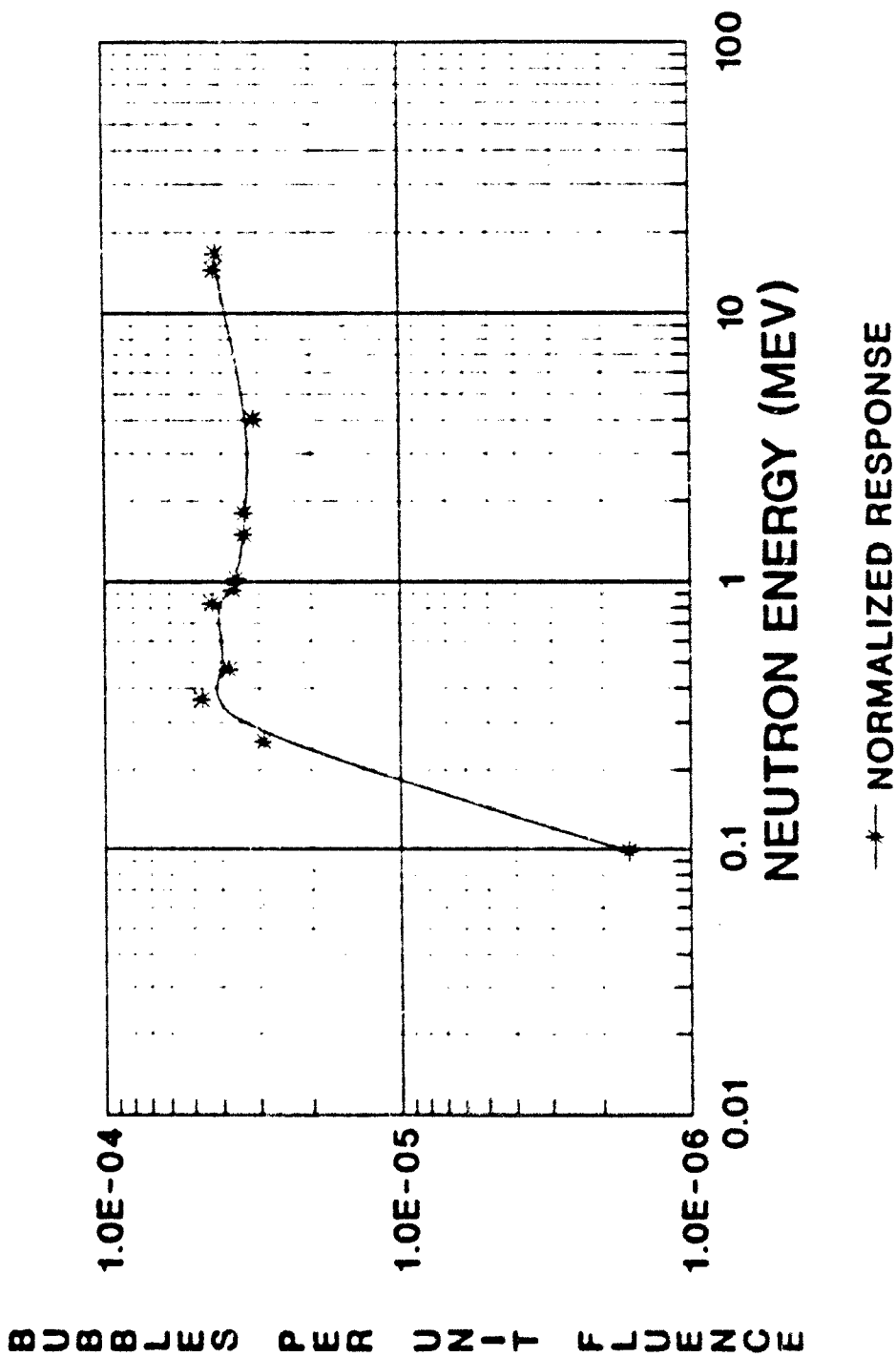
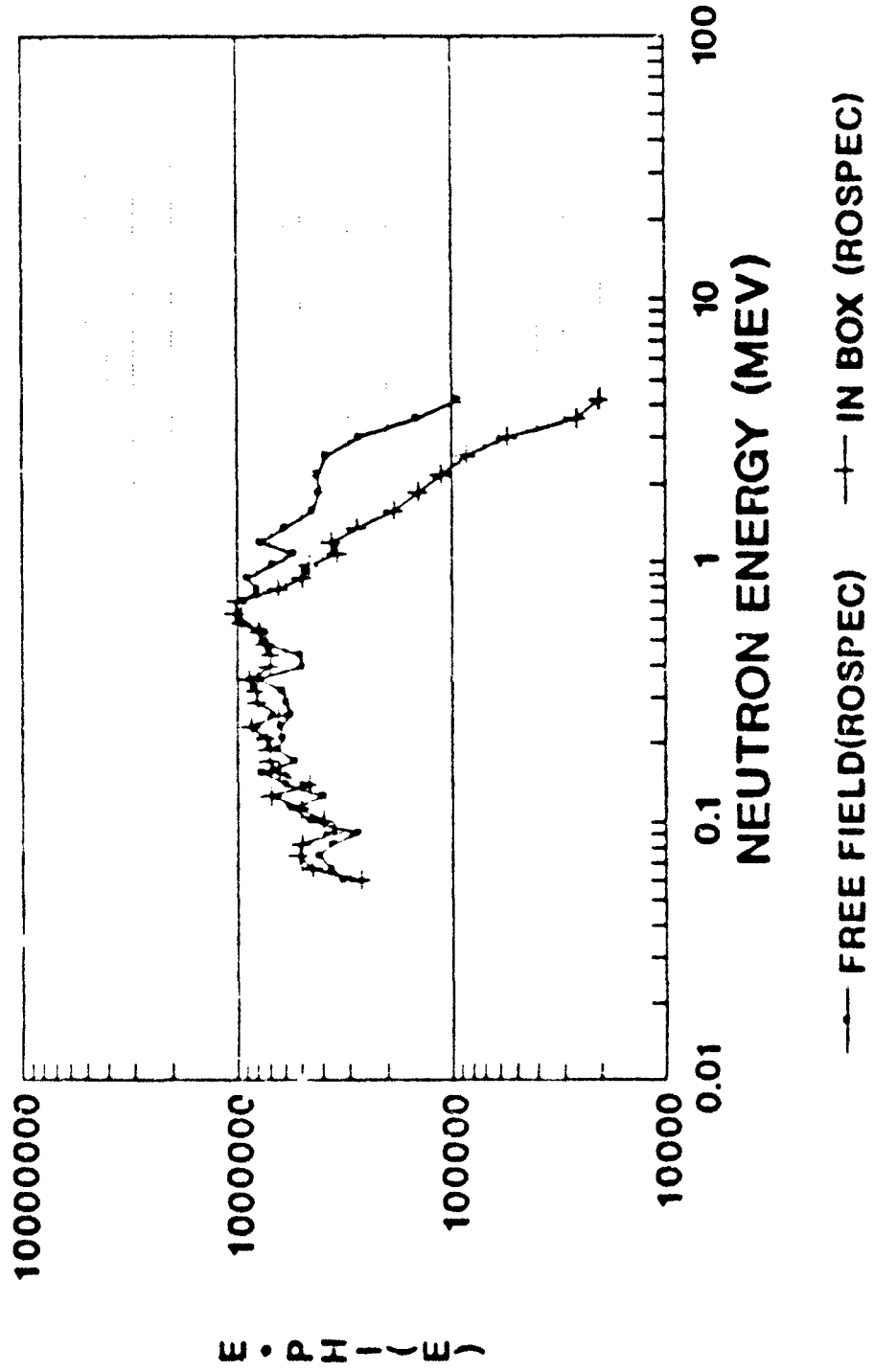


FIGURE 2 2D100R fluence/energy response used in this report.

FF AND IN BOX NEUTRON SPECTRA



NORMALIZED PER KWH

FIGURE 3 Measured (ROSPEC) neutron energy spectra both free-field (at the NATO standard reference point) and in the test bed configuration.

TISSUE AND SI DISPLACEMENT KERMA

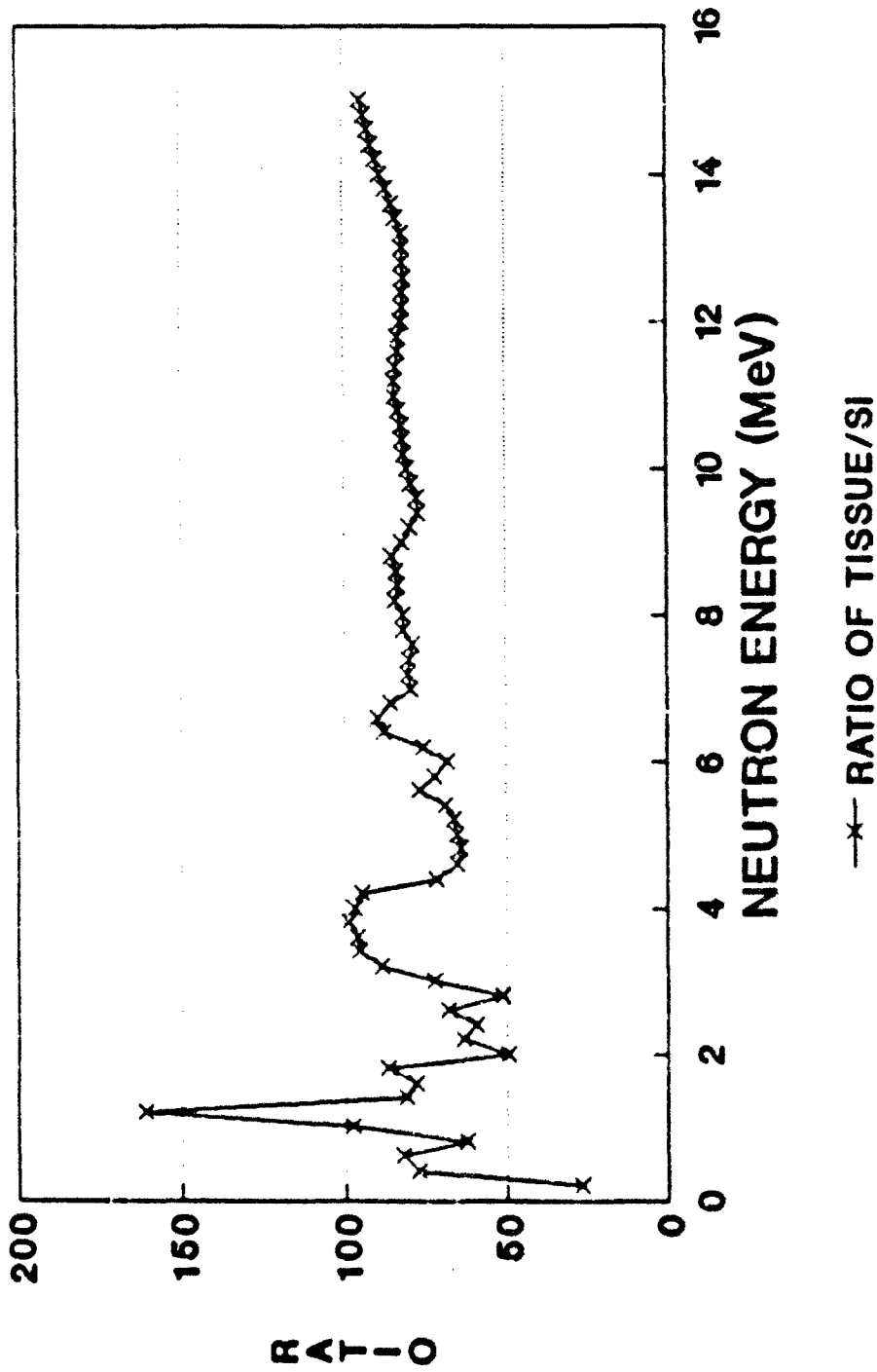


FIGURE 4 Ratio of neutron tissue kerma to neutron displacement kerma in Si. Note the structure riding on a fairly flat base.

VPF/ATR FREE-FIELD CALCULATIONS ITI RANGE

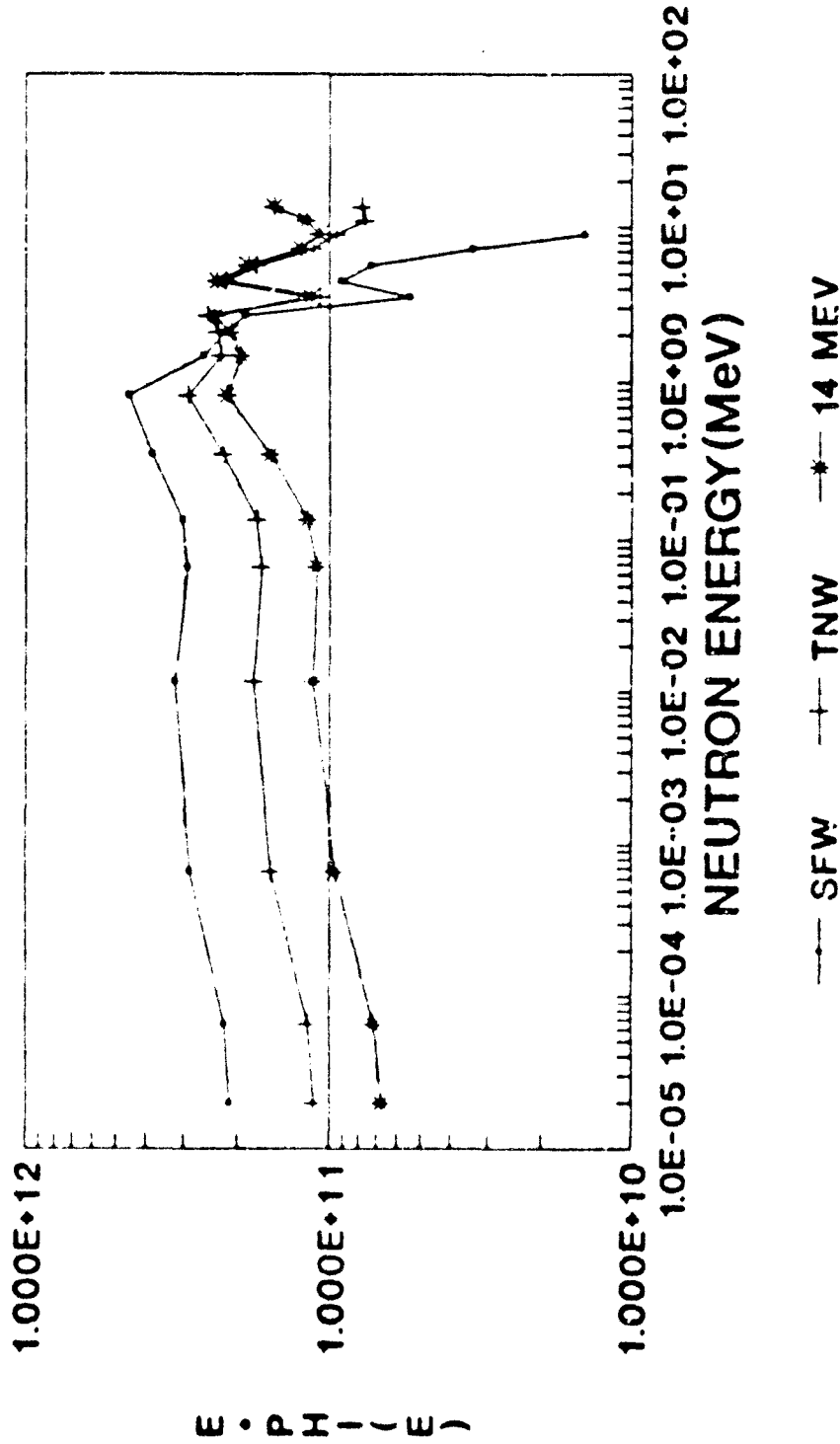
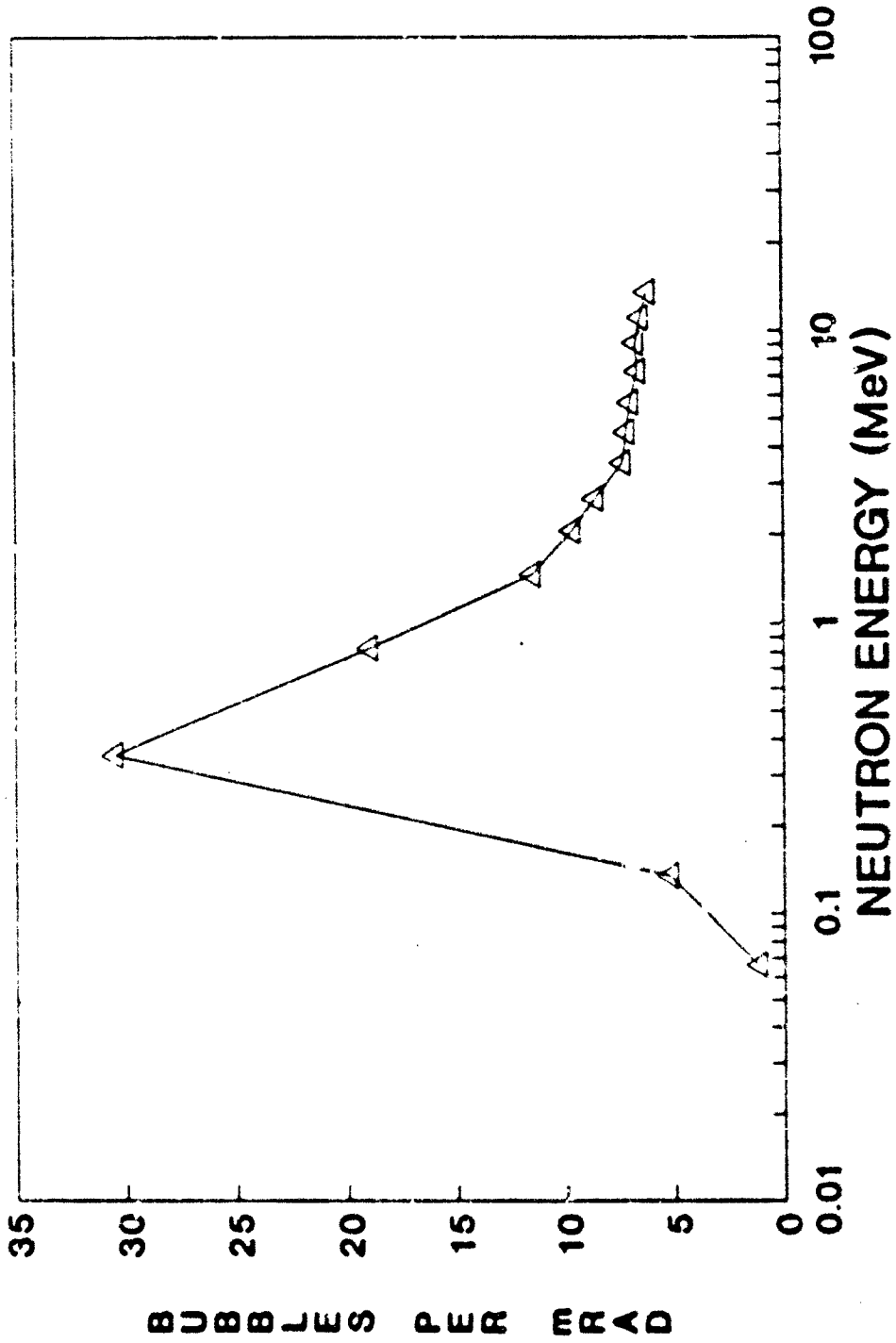


FIGURE 5 Free field neutron energy spectra (for the ITI case) as calculated by ATR5 for the three weapon scenarios.

BD100R / TISSUE KERMA RESPONSE



MEASURED AT DREO VAN DE GRAAFF

FIGURE 6 Ratio of bubble response per neutron tissue kerma showing a large peak in the area of 300-400 keV.

6 INCH STEEL VEHICLE EFFECT ON THERMONUCLEAR SPECTRUM

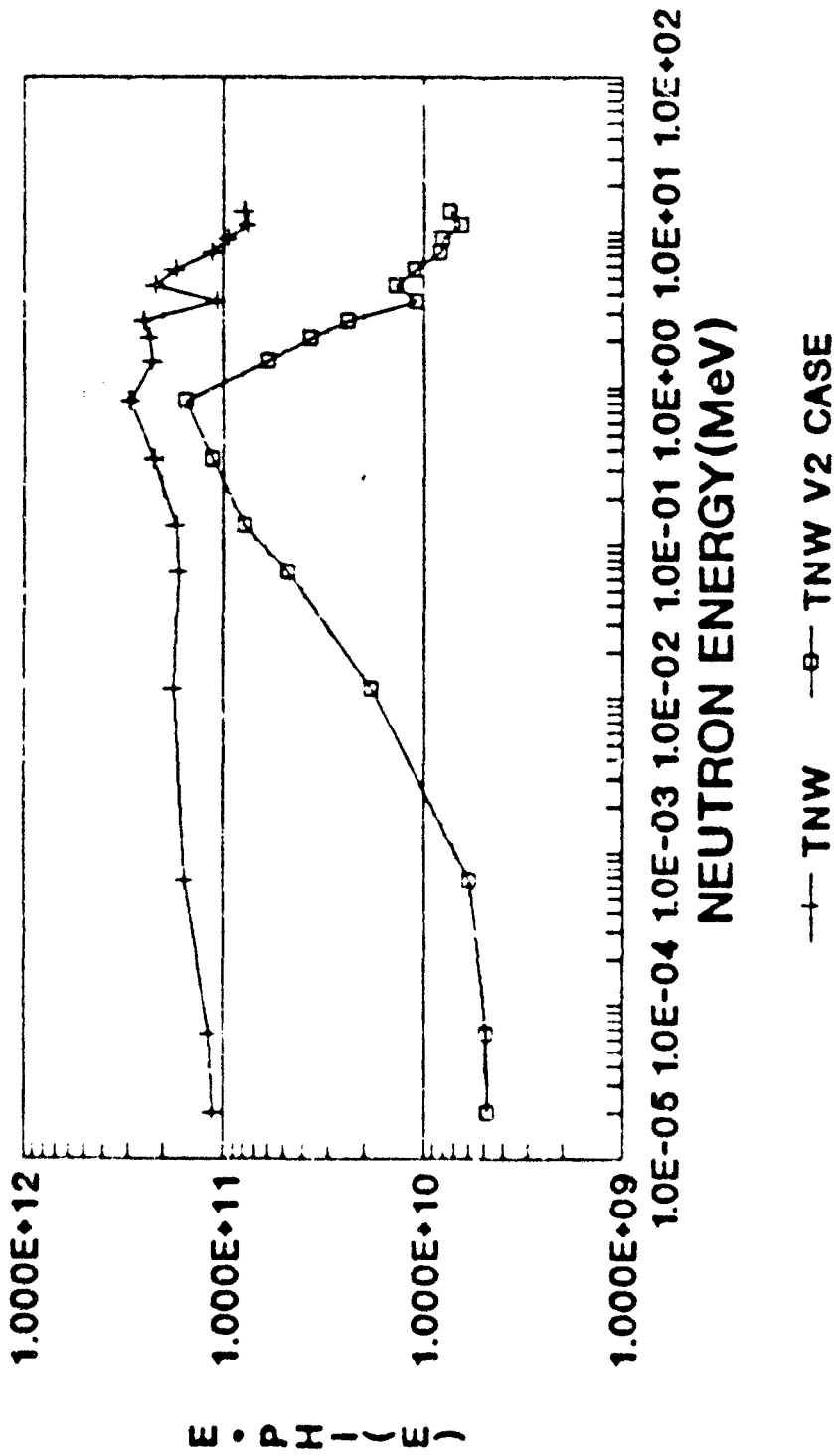


FIGURE 7 Free-field (ITI) and V2 neutron energy spectra for the TNW scenario as calculated by VPF2. Note the maximum in the V2 spectra is a roughly the same energy as the peak in the bubble per tissue kerma curve (Figure 6). This is responsible for the high values for bubble detector measured kerma predicted in the text.

Appendix A

SOURCE SPECTRA USED IN THIS REPORT

| CASE | Energy Boundaries (MeV) | SFW (Fraction in Group) | TNW (Fraction in Group) |
|-------|----------------------------|---|----------------------------|
| | Group | | |
| | 1 | $1.07 \times 10^{-5} - 2.90 \times 10^{-5}$ | 0 |
| | 2 | $2.9 \times 10^{-5} - 1.01 \times 10^{-4}$ | 0 |
| | 3 | $1.01 \times 10^{-4} - 1.23 \times 10^{-3}$ | 0 |
| | 4 | $1.23 \times 10^{-3} - 2.19 \times 10^{-2}$ | 0.01649 |
| | 5 | $2.19 \times 10^{-2} - 1.11 \times 10^{-1}$ | 0.20617 |
| N | 6 | .111 - .158 | 0.01799 |
| E | 7 | .158 - .550 | 0.15129 |
| U | 8 | .55 - 1.11 | 0.21587 |
| T | 9 | 1.11 - 1.83 | 0.14678 |
| R | 10 | 1.83 - 2.31 | 0.10173 |
| O | 11 | 2.31 - 3.01 | 0.03871 |
| N | 12 | 3.01 - 4.07 | 0.0548 |
| S | 13 | 4.07 - 4.97 | 0.01177 |
| | 14 | 4.97 - 6.36 | 0.01832 |
| | 15 | 6.36 - 8.19 | 0.01274 |
| | 16 | 8.19 - 10.0 | 0.00734 |
| | 17 | 10.0 - 12.2 | 0 |
| | 18 | 12.2 - 15.0 | 0 |
| <hr/> | | | |
| | 1 | 0.01 - 0.045 | 0.03259 |
| | 2 | 0.045 - 0.10 | 0.01644 |
| | 3 | 0.10 - 0.15 | 0.04881 |
| | 4 | 0.15 - 0.30 | 0.10321 |
| | 5 | 0.30 - 0.45 | 0.13571 |
| G | 6 | 0.45 - 0.70 | 0.20256 |
| A | 7 | 0.70 - 1.00 | 0.16332 |
| M | 8 | 1.00 - 1.5 | 0.14073 |
| M | 9 | 1.5 - 2.0 | 0.06429 |
| A | 10 | 2.0 - 2.5 | 0.03743 |
| - | 11 | 2.5 - 3.0 | 0.02225 |
| R | 12 | 3.0 - 4.0 | 0.02109 |
| A | 13 | 4.0 - 5.0 | 0.00746 |
| Y | 14 | 5.0 - 6.0 | 0.00265 |
| S | 15 | 6.0 - 7.0 | 0.00092 |
| | 16 | 7.0 - 8.0 | 0.00038 |
| | 17 | 8.0 - 10.0 | 0.00016 |
| | 18 | 10.0 - 12.0 | 0 |

Appendix B

SAMPLE OF CALCULATIONAL RESULTS
(ABBREVIATIONS EXPLAINED IN TEXT)

| Group | Mean Neutron Energy (MeV) | SFW/5kT/LD50/FF Fluence in Group (n/cm ²) | SFW/5kT/LD50/V1 Fluence in Group (n/cm ²) |
|-------|---------------------------|---|---|
| 1 | 1.99×10^{-5} | 3.64×10^{10} | 3.14×10^{10} |
| 2 | 6.50×10^{-5} | 4.52×10^{10} | 3.91×10^{10} |
| 3 | 6.65×10^{-4} | 8.94×10^{10} | 7.36×10^{10} |
| 4 | 1.16×10^{-2} | 1.04×10^{11} | 8.74×10^{10} |
| 5 | 6.64×10^{-2} | 7.07×10^{10} | 4.65×10^{10} |
| 6 | 1.35×10^{-1} | 1.89×10^{10} | 1.45×10^{10} |
| 7 | 3.54×10^{-1} | 7.42×10^{10} | 4.85×10^{10} |
| 8 | 8.30×10^{-1} | 5.24×10^{10} | 4.08×10^{10} |
| 9 | 1.47 | 2.17×10^{10} | 1.71×10^{10} |
| 10 | 2.07 | 9.30×10^9 | 7.59×10^9 |
| 11 | 2.66 | 9.55×10^9 | 6.48×10^9 |
| 12 | 3.54 | 3.01×10^9 | 2.42×10^9 |
| 13 | 4.52 | 4.19×10^9 | 2.90×10^9 |
| 14 | 5.67 | 3.76×10^9 | 2.38×10^9 |
| 15 | 7.28 | 1.70×10^9 | 9.97×10^8 |
| 16 | 9.10 | 5.47×10^8 | 3.01×10^8 |
| 17 | 11.1 | 0 | 0 |
| 18 | 13.6 | 0 | 0 |

Appendix B (Continued)

SAMPLE OF CALCULATIONAL RESULTS
(ABBREVIATIONS EXPLAINED IN TEXT)

| Group | Mean Neutron Energy (MeV) | TNW/5kT/ITI/FF Fluence in Group (n/cm ²) | TNW/5kT/ITI/V2 Fluence in Group (n/cm ²) |
|-------|------------------------------|--|--|
| 1 | 1.99 x 10 ⁻³ | 1.05 x 10 ¹¹ | 4.41 x 10 ⁹ |
| 2 | 6.50 x 10 ⁻³ | 1.31 x 10 ¹¹ | 5.38 x 10 ⁹ |
| 3 | 6.65 x 10 ⁻⁴ | 2.64 x 10 ¹¹ | 1.00 x 10 ¹⁰ |
| 4 | 1.16 x 10 ⁻² | 3.17 x 10 ¹¹ | 3.26 x 10 ¹⁰ |
| 5 | 6.64 x 10 ⁻² | 2.24 x 10 ¹¹ | 6.38 x 10 ¹⁰ |
| 6 | 1.35 x 10 ⁻¹ | 6.03 x 10 ¹⁰ | 2.72 x 10 ¹⁰ |
| 7 | 3.54 x 10 ⁻¹ | 2.47 x 10 ¹¹ | 1.26 x 10 ¹¹ |
| 8 | 8.30 x 10 ⁻¹ | 1.96 x 10 ¹¹ | 1.04 x 10 ¹¹ |
| 9 | 1.47 | 1.11 x 10 ¹¹ | 2.91 x 10 ¹⁰ |
| 10 | 2.07 | 5.38 x 10 ¹⁰ | 8.42 x 10 ⁹ |
| 11 | 2.66 | 6.61 x 10 ¹⁰ | 6.22 x 10 ⁹ |
| 12 | 3.54 | 3.20 x 10 ¹⁰ | 3.24 x 10 ⁹ |
| 13 | 4.52 | 4.37 x 10 ¹⁰ | 2.70 x 10 ⁹ |
| 14 | 5.67 | 4.25 x 10 ¹⁰ | 2.70 x 10 ⁹ |
| 15 | 7.28 | 2.84 x 10 ¹⁰ | 2.05 x 10 ⁹ |
| 16 | 9.10 | 1.88 x 10 ¹⁰ | 1.58 x 10 ⁹ |
| 17 | 11.1 | 1.51 x 10 ¹⁰ | 1.29 x 10 ⁹ |
| 18 | 13.6 | 1.61 x 10 ¹⁰ | 1.50 x 10 ⁹ |

Appendix B (Continued)

SAMPLE OF CALCULATIONAL RESULTS
(ABBREVIATIONS EXPLAINED IN TEXT)

| Group | Mean Neutron Energy (MeV) | 14 MeV/100kT/ITI/FF Fluence in Group | 14 MeV/100kT/ITI/V4 Fluence in Group |
|-------|---------------------------|--------------------------------------|--------------------------------------|
| 1 | 1.99×10^{-5} | 6.77×10^{10} | 3.79×10^9 |
| 2 | 6.50×10^{-5} | 8.57×10^{10} | 4.66×10^9 |
| 3 | 6.65×10^{-4} | 1.74×10^{11} | 9.22×10^9 |
| 4 | 1.16×10^{-2} | 2.14×10^{11} | 1.07×10^{10} |
| 5 | 6.64×10^{-2} | 1.50×10^{11} | 7.62×10^9 |
| 6 | 1.35×10^{-1} | 4.55×10^{10} | 2.28×10^9 |
| 7 | 3.54×10^{-1} | 1.89×10^{11} | 1.07×10^{10} |
| 8 | 8.30×10^{-1} | 1.54×10^{11} | 9.56×10^9 |
| 9 | 1.47 | 9.07×10^{10} | 5.24×10^9 |
| 10 | 2.07 | 4.93×10^{10} | 2.04×10^9 |
| 11 | 2.66 | 6.61×10^{10} | 1.83×10^9 |
| 12 | 3.54 | 3.47×10^{10} | 1.53×10^9 |
| 13 | 4.52 | 5.40×10^{10} | 1.53×10^9 |
| 14 | 5.67 | 4.88×10^{10} | 1.55×10^9 |
| 15 | 7.28 | 3.33×10^{10} | 1.30×10^9 |
| 16 | 9.10 | 2.23×10^{10} | 1.03×10^9 |
| 17 | 11.1 | 1.85×10^{10} | 8.77×10^8 |
| 18 | 13.6 | 1.87×10^{10} | 9.65×10^8 |

5. BIBLIOGRAPHY

1. NATO Allied Engineering Publication- AEP-14 - 'Guidelines for the Armoured Fighting Vehicle Designer to Improve Radiation Protection (U)' (CONFIDENTIAL).
2. '1987 Annual Book of ASTM Standards - Section 12; Nuclear, Solar and Geothermal Energy' E722-85, p442, American Society for Testing and Materials, Philadelphia, 1987.
3. Namenson A.I., E.A. Wolicki and G.C. Messenger, 'Neutron Displacement Kerma Factor at 1 MeV' IEEE Trans Nuc Sci, NS-29, No 1, 1982, pp 1018-1020.
4. Jamieson T.J. and T. Cousins, 'VPF-2 - Version 2 of a Simplified Code for Radiation Protection Calculation' presented at NATO RSG-5 (Panel VIII) Physical Dosimetry Sub-Committee Meeting, Paris, April, 1989 (to be published).
5. 'ATRS: Models of Radiation Transport in Air - the ATR Code', Oak Ridge National Laboratory, Radiation Information Shielding Centre, Report CCC-179.
6. Cousins T., 'The Use of the Computer Code ATR to Relate DREO Experimental Results to Nuclear Battlefield Threats' DREO Technical Note 89-10, February, 1989.
7. Kazi A.H., T. Cousins and D.M. Eagleson '1986 NATO Battlefield Dosimeter Intercomparison Data Summary' USA CSTA Technical Report No. 6487, Feb 1987.
8. Ing H. and T. Cousins 'Possible Use of the Bubble Dosimeter for Battlefield Requirements' presented at NATO RSG-5 (Panel VIII) Physical Dosimetry Sub-Committee Meeting, Paris, April, 1989 (to be published).
9. McGowan M.S., DREO, private communication.
10. Ing H., Bubble Technology Industries, private communication.
11. Cousins T., B.E. Hoffarth, H. Ing and K. Tremblay 'Recent Re-measurements of the Neutron and Gamma-ray Fields at Large Distances from a Prompt Critical Facility' DREO report (in press).
12. Kazi A.H. 'Future Collaborative Work at APG' presented at NATO RSG-5 (Panel VIII) Physical Dosimetry Sub-Committee Meeting, Paris, April, 1989 (to be published).
13. Cousins T. and T.J. Jamieson 'Summary of Results of NATO Dosimetry Sub-Committee Computer Intercomparison Study' presented at NATO RSG-5 (Panel VIII) Physical Dosimetry Sub-Committee Meeting, Paris, April, 1989 (to be published).

SECURITY CLASSIFICATION OF FORM
(highest classification of Title, Abstract, Keywords)

| DOCUMENT CONTROL DATA | | |
|---|---|---|
| (Security classification of title, body of abstract and indexing annotation must be entered when the overall document is classified) | | |
| 1. ORIGINATOR (the name and address of the organization preparing the document. Organizations for whom the document was prepared, e.g. Establishment sponsoring a contractor's report, or tasking agency, are entered in section 8.) Defence Research Establishment Ottawa Ottawa, Ontario K1A 0Z4 | 2. SECURITY CLASSIFICATION (overall security classification of the document, including special warning terms if applicable) UNCLASSIFIED | |
| 3. TITLE (the complete document title as indicated on the title page. Its classification should be indicated by the appropriate abbreviation (S,C,R or U) in parentheses after the title.) The Validity of the Use of the Neutron Reduction Factor in Assessing Displacement Damage to Electronics In Armoured Vehicles (U) | | |
| 4. AUTHORS (Last name, first name, middle initial) Cousins, Thomas and Jamieson, Terrence J. | | |
| 5. DATE OF PUBLICATION (month and year of publication of document) February 1990 | 6a. NO. OF PAGES (total containing information. Include Annexes, Appendices, etc.) 33 | 6. NO. OF REFS (total cited in document) 13 |
| 7. DESCRIPTIVE NOTES (the category of the document, e.g. technical report, technical note or memorandum. If appropriate, enter the type of report, e.g. interim, progress, summary, annual or final. Give the inclusive dates when a specific reporting period is covered.) DREO Report | | |
| 8. SPONSORING ACTIVITY (the name of the department project office or laboratory sponsoring the research and development. Include the address.) Defence Research Establishment Ottawa Ottawa, Ontario K1A 0Z4 | | |
| 9a. PROJECT OR GRANT NO. (if appropriate, the applicable research and development project or grant number under which the document was written. Please specify whether project or grant) 041LS | 9b. CONTRACT NO. (if appropriate, the applicable number under which the document was written) | |
| 10a. ORIGINATOR'S DOCUMENT NUMBER (the official document number by which the document is identified by the originating activity. This number must be unique to this document.) DREO Report 1032 | 10b. OTHER DOCUMENT NOS. (Any other numbers which may be assigned this document either by the originator or by the sponsor) | |
| 11. DOCUMENT AVAILABILITY (any limitations on further dissemination of the document, other than those imposed by security classification) <input checked="" type="checkbox"/> Unlimited distribution <input type="checkbox"/> Distribution limited to defence departments and defence contractors; further distribution only as approved <input type="checkbox"/> Distribution limited to defence departments and Canadian defence contractors; further distribution only as approved <input type="checkbox"/> Distribution limited to government departments and agencies; further distribution only as approved <input type="checkbox"/> Distribution limited to defence departments; further distribution only as approved <input type="checkbox"/> Other (please specify): | | |
| 12. DOCUMENT ANNOUNCEMENT (any limitation to the bibliographic announcement of this document. This will normally correspond to the Document Availability (11). However, where further distribution beyond the audience specified in 11) is possible, a wider announcement audience may be selected.) | | |

UNCLASSIFIED

SECURITY CLASSIFICATION OF FORM

13. ABSTRACT (a brief and factual summary of the document. It may also appear elsewhere in the body of the document itself. It is highly desirable that the abstract of classified documents be unclassified. Each paragraph of the abstract shall begin with an indication of the security classification of the information in the paragraph (unless the document itself is unclassified) represented as (S), (C), (R), or (U). It is not necessary to include here abstracts in both official languages unless the text is bilingual).

The degree of protection from neutron irradiation afforded to electronics by armoured vehicles is most currently defined by the outside-to-inside ratio of the 1 MeV equivalent neutron fluence for Silicon. It has been proposed that this factor may be approximated by an experimentally measurable parameter - the neutron (tissue kerma) reduction factor. This report examines the validity of this assumption for a variety of realistic nuclear battlefield scenarios, calculated using the computer code VPF2. In addition the response of two neutron dosimeters in the calculated fields is examined.

14. KEYWORDS, DESCRIPTORS or IDENTIFIERS (technically meaningful terms or short phrases that characterize a document and could be helpful in cataloguing the document. They should be selected so that no security classification is required. Identifiers, such as equipment model designation, trade name, military project code name, geographic location may also be included. If possible keywords should be selected from a published thesaurus, e.g. Thesaurus of Engineering and Scientific Terms (TEST) and that thesaurus-identified. If it is not possible to select indexing terms which are Unclassified, the classification of each should be indicated as with the title.)

Neutron
Nuclear Radiation
Radiation Protection
Silicon Displacement Damage
Radiation Transport
Computer Codes
Nuclear Weapons

Canadian Forces

UNCLASSIFIED

SECURITY CLASSIFICATION OF FORM